Article

# A Conclusive Mechanism of the Photoinduced Reaction Cascade in Blue Light Using Flavin Photoreceptors

Keyarash Sadeghian, Marco Bocola, and Martin Schu#tz

*J. Am. Chem. Soc.*, **2008**, 130 (37), 12501-12513 • DOI: 10.1021/ja803726a • Publication Date (Web): 23 August 2008



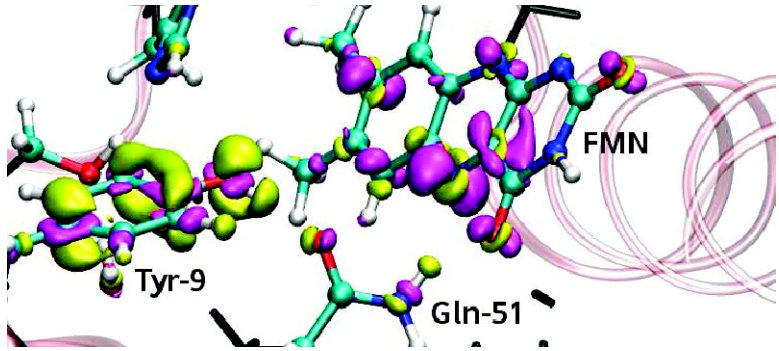


## More About This Article

Additional resources and features associated with this article are available within the HTML version:

- Supporting Information
- Access to high resolution figures
- Links to articles and content related to this article
- Copyright permission to reproduce figures and/or text from this article

View the Full Text HTML

J|A|C|S
ARTICLES

Published on Web 08/23/2008

# A Conclusive Mechanism of the Photoinduced Reaction Cascade in Blue Light Using Flavin Photoreceptors

Keyarash Sadeghian,[†] Marco Bocola,[‡] and Martin Schütz*,[†]

*Institute of Physical and Theoretical Chemistry, and Institute of Biophysics and Physical Biochemistry, University of Regensburg, Universitätsstrasse 31, D-93040 Regensburg, Germany*

Received May 23, 2008; E-mail: martin.schuetz@chemie.uni-regensburg.de

***Abstract:*** On the basis of extensive first-principle calculations within the framework of quantum mechanics/molecular mechanics (QM/MM), a conclusive mechanism for the formation of the signaling state of blue light using flavin (BLUF) domain proteins is proposed which is compatible with the experimental data presently available. Time-dependent density functional, as well as advanced coupled cluster response theory was employed for the QM part in order to describe the relevant excited states. One of the key residues involved in the mechanism is the glutamine adjacent to the flavin chromophore. The reaction cascade, triggered by the initial photoexcitation of the flavin chromophore, involves isomerization of this residue but no rotation as assumed previously. The fact that only the environment, but not the flavin chromophore by itself, is chemically transformed along the individual steps of the mechanism is unique for biological photoreceptors. The final isomer of the glutamine tautomer, i.e., the imidic acid, is further stabilized by the interchange of a methionine residue in the binding pocket with a tryptophan residue. The flip of these two residues might be the trigger for the large conformational change of this protein which is consequently transmitted as the signal to the biological environment.

## 1. Introduction

The ability of organisms to adapt to environmental conditions, such as light, is the key to their survival and further development. For this purpose they require a suitable machinery at the molecular level to sense both the amount and type of exposed light. A reliable and nevertheless flexible mechanism is then required for the final transduction of the consequently formed signal. Bacteria, plants, and mammals use biological photoreceptors to perceive light from different parts of the visible spectrum, as regulatory components for vital processes such as growth, development, color vision, circadian rhythms, and photomovement.[1]

Depending on the photoactive chromophore and the initial steps in the photochemical process(es) found or postulated for these photoreceptors, they can be divided into six different families:[2] rhodopsins,[3] phytochromes,[4] xanthopsins,[5] phototropins,[6−9] cryptochromes,[10] and BLUF (blue light using flavin adenine dinucleotide FAD) proteins.[11] The main chromophores in the first three families, namely retinal, phytochromobilin, and *p*-coumaric acid, respectively, undergo cis/trans isomerization upon excitation. The last three groups all have flavin as their light-sensitive chromophore, but the mechanism for the signal transfer from the excited chromophore to the surroundings is not yet fully understood. In the case of the light−oxygen−voltage (LOV) domains, belonging to the phototropin family, an intersystem crossing process followed by the formation of a covalent Cys adduct is believed to trigger the biological signal.[12,13] For the cryptochrome family a (reversible) electron-transfer process has been proposed.[14,15]

The first BLUF domain, which is the subject of this study, was discovered in a flavoprotein AppA, a transcriptional antirepressor from the purple photosynthetic bacterium *Rhodobacter sphaeroides* and was shown to control photosynthesis gene expression depending on blue-light and/or oxygen conditions.[16] Since then several BLUF signaling domains have been found in prokaryotic and eukaryotic microorganisms all having common spectroscopic features for their signaling state (see below), although having different physiological functions such

[†] Institute of Physical and Theoretical Chemistry.
[‡] Institute of Biophysics and Physical Chemistry.

(1) Christie, J. M.; Briggs, W. R. *J. Biol. Chem.* **2001**, *276*, 11457.
(2) van der Horst, M. A.; Hellingwerf, K. J. *Acc. Chem. Res.* **2004**, *37*, 13.
(3) Hoff, W. D.; Jung, K. H.; Spudlich, J. L. *Annu. Rev. Biophys. Biomol. Struct.* **1997**, *26*, 223.
(4) Quail, P. H. *Philos. Trans. R. Soc. London, Ser. B* **1998**, *353*, 1399.
(5) Kort, R.; Hoff, W. D.; van West, M.; Kroon, A. R.; Hoffer, S. M.; Vlieg, K. H.; Crielaand, W.; Beeumen, J. J. V.; Hellingwerf, K. J. *EMBO J.* **1996**, *15*, 3209.
(6) Huala, E.; Oeller, P. W.; Liscum, E.; Han, I. S.; Larsen, E.; Briggs, W. R. *Science* **1997**, *278*, 2120.
(7) Swartz, T. E.; Corchnoy, S. B.; Christie, J. M.; Lewis, J. W.; Szundi, I.; Briggs, W. R.; Bogomolni, R. A. *J. Biol. Chem.* **2001**, *276*, 36493.
(8) Crosson, S.; Moffat, K. *Proc. Natl. Acad. Sci. U.S.A.* **2001**, *98*, 2995.
(9) Holzer, W.; Penzkofer, A.; Fuhrmann, M.; Hegemann, P. *Photochem. Photobiol.* **2002**, *75*, 479.
(10) Ahmad, M.; Cashmore, A. R. *Nature* **1993**, *366*, 162.
(11) Gomelsky, M.; Klug, G. *Trends Biochem. Sci.* **2002**, *27*, 497.
(12) Kottke, T.; Heberle, J.; Hehn, D.; Dick, B.; Hegemann, P. *Biophys. J.* **2003**, *84*, 1192.
(13) Briggs, W.; et al. *Plant Cell* **2001**,*13*, 993.
(14) Lin, C. *Trends Plant Sci.* **2000**, *5*, 337.
(15) Cashmore, A.; Jarillo, J. A.; Wu, Y.-J.; Liu, D. *Science* **1999**, *284*, 760.
(16) Masuda, S.; Bauer, C. *Cell* **2002**, *110*, 613.

  

as photophobic response in photoactivated adenylyl cyclase (PAC) of *Euglena gracilis*.[17]

Apart from large conformational changes which lead to the biological signal, an interesting and so far not fully understood aspect of such a receptor domain is the extent and nature of the slight and yet profound conformational changes in the FAD chromophore and its neighborhood upon blue-light illumination. In the case of BLUF domains the absorption spectra of the photoinduced (signaling) state is only 10 nm red-shifted compared to the dark-adapted (receptor) state[16] stressing the fact that the chromophore itself does not change its conformation as such. This indeed is the common feature of all BLUF domains known to this date as is evident from the extensive spectroscopy measurements carried out on AppA,[18−22] BlrB,[23,24] Slr1694,[25−28] and Tll0078[29−31] so far. The signaling state, which remains stable for minutes,[16] is formed within 1 ns[32,33] after photoexcitation without an intermediate which is stable at room temperature. The hydrogen-bonding network associated with this orientation proves to be crucial for the signaling state formation. FT-IR and Raman spectroscopy measurements carried out on the dark- and light-adapted states AppA,[34] Slr1694,[27] and Tll0078[31] show a 10 $cm^{-1}$ red-shift in the stretch mode assigned to the C4═O4 carbonyl group of flavin mononucleotide (FMN, see Figure 1). This result is interpreted as the formation of a stronger hydrogen bond at O4 position of the flavin chromophore in the signaling state.

A conclusive mechanism for the signaling state formation in BLUF domains is complicated by the fact that there is no unique crystal structure available for either the dark or the signaling state. There is some ambiguity regarding the position and/or orientation of the Gln-51, Trp-92, and Met-94 with respect to the flavin moiety. (cf., Figure 2, the numbering throughout this paper is taken from the crystal structure of BlrB).[23]

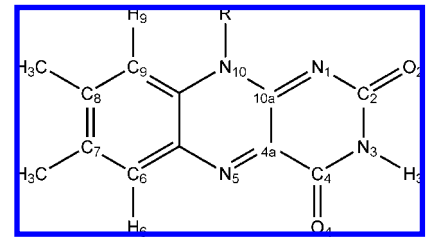


***Figure 1.*** Isoalloxazine ring of FMN.

An electron-transfer process from Tyr-9 to FMN has been proposed to be responsible for the fluorescence quenching of the flavin moiety.[19,28,31,36−39] A mechanism postulated by Gauden et al. involves a light-driven electron and proton transfer from Tyr to FAD followed by a hydrogen-bonding network rearrangement in AppA[22] and Slr1694 mainly due to the rotation of Gln.[32] Recently Domratcheva et al. postulated the possibility of Gln rotation during the lifetime of the biradical state of the system[40] which is then followed by biradical recombination leading to the tautomeric form of Gln-51. The possibility of tautomerization was proposed earlier in the FT-IR study of Stelling et al. on AppA.[41]

In this study we present a plausible mechanism for the formation of the signaling state after the initial photoexcitation based on extensive quantum mechanics/molecular mechanics (QM/MM) calculations (for a recent review see ref 42) with appropriate QM methods describing ground- and electronically excited states. In these calculations the FMN chromophore, along with its nearest neighboring amino acids, were treated quantum mechanically (QM part), whereas the remaining protein environment was treated at the level of a classical force field (MM part). The effect of the MM environment enters the QM Hamiltonian at the level of distributed point charges. There is strong evidence that, after photoexcitation of a locally excited (LE) state, the Tyr-9−FMN charge-transfer (CT) state is populated via a conical intersection. Our calculations show that the downhill path on this CT surface then leads via a further conical intersection with the closed-shell ground state to the biradical species ($Tyr^{\bullet}$−$flavin^{\bullet}$), hence confirming the experimental results from the theoretical perspective. Furthermore, possible channels for the recombination of the biradical are explored. The barrier for the process involving rotation of the Gln-51 in the presence of $Tyr^{\bullet}$ and $flavin^{\bullet}$ is compared to the barrier for rotation-free direct radical recombination to Gln-oxygen (see Figure 8). The latter possibility has not been considered so far, yet it is demonstrated in this work that it is more compatible with the short lifetimes observed in spectroscopy measurements than alternative recombination mechanisms.

(17) Iseki, M.; Matsunaga, S.; Murakami, A.; Ohno, K.; Shiga, K.; Yoshida, K.; Sugai, M.; Takahashi, T.; Hori, T.; Watanabe, M. *Nature* **2002**, *415*, 1047.
(18) Laan, W.; van der Horst, M. A.; van Stokkum, I. H.; Hellingwerf, K. J. *Photochem. Photobiol.* **2003**, *78*, 290.
(19) Dragnea, V.; Waegele, M.; Balascuta, S.; Bauer, C.; Dragnea, B. *Biochemistry* **2005**, *44*, 15978.
(20) Masuda, S.; Hasegawa, K.; Ono, T.-A. *Biochemistry* **2005**, *44*, 1215.
(21) Zirak, P.; Penzkofer, A.; Schiereis, T.; Hegemann, P.; Jung, A.; Schlichting, I. *Chem. Phys.* **2005**, *315*, 142.
(22) Gauden, M.; Grinstead, J. S.; Laan, W.; van Stokkum, I. H. M.; Avila-Perez, M.; Toh, K.; Boelens, R.; Kapstein, R.; van Grondelle, R.; Hellingwerf, K. J.; Kennis, J. T. M. *Biochemistry* **2007**, *46*, 7405.
(23) Jung, A.; Domratcheva, T.; Tarutina, M.; Wu, Q.; Ko, W.-H.; Shoeman, R.; Gomelsky, M.; Gardner, K. H.; Schlichting, I. *Proc. Natl. Acad. Sci. U.S.A.* **2005**, *102*, 12350.
(24) Zirak, P.; Penzkofer, A.; Hegemann, T. S. P.; Jung, A.; Schlichting, I. *Photochem. Photobiol., B* **2006**, *83*, 180.
(25) Yuan, H.; Anderson, S.; Masuda, S.; Dragnea, V.; Moffat, K.; Bauer, C. *Biochemistry* **2006**, *45*, 12687.
(26) Hasegawa, K.; Masuda, S.; Ono, T.-A. *Biochemistry* **2004**, *43*, 14979.
(27) Masuda, S.; Hasegawa, K.; Ishii, A.; Ono, T.-A. *Biochemistry* **2004**, *43*, 5304.
(28) Zirak, P.; Penzkofer, A.; Lehmpfuhl, C.; Mathes, T.; Hegemann, P. *Photochem. Photobiol., B* **2007**, *86*, 22.
(29) Kita, A.; Okajima, K.; Morioto, Y.; Ikeuchi, M.; Miki, K. *J. Mol. Biol.* **2005**, *349*, 1.
(30) Fukushima, Y.; Okajima, K.; Shibata, Y.; Ikeuchi, M.; Itoh, S. *Biochemistry* **2005**, *44*, 5149.
(31) Okajima, K.; Fukushima, Y.; Suzuki, H.; Kita, A.; Ochiai, Y.; Katayama, M.; Shibata, Y.; Miki, K.; Noguchi, T.; Itoh, S.; Ikeuchi, M. *J. Mol. Biol.* **2006**, *363*, 10.
(32) Gauden, M.; van Stokkum, I. H. M.; Key, J. M.; Lührs, D. C.; van Grondelle, R.; Hegemann, P.; Kennis, J. T. M. *Proc. Natl. Acad. Sci. U.S.A.* **2006**, *103*, 10895.
(33) Laan, W.; Gauden, M.; Yeremenko, S.; van Grondelle, R.; Kennis, J. T. M.; Hellingwerf, K. J. *Biochemistry* **2006**, *45*, 51.
(34) Unno, M.; Sano, R.; Masuda, S.; Ono, T.-A.; Yamauchi, S. *J. Phys. Chem. B* **2005**, *109*, 12620.
(35) Anderson, S.; Dragnea, V.; Masuda, S.; Ybe, J.; Moffat, K.; Bauer, C. *Biochemistry* **2005**, *44*, 7998.
(36) Laan, W.; van der Horst, M.; van Stokkum, I.; Hellingwerf, K. *Photochem. Photobiol.* **2003**, *78*, 290.
(37) Zirak, P.; Penzkofer, A.; Hegemann, P.; Mathes, T. *Chem. Phys.* **2007**, *335*, 15.
(38) Kraft, B. J.; Masuda, S.; Kikuchi, J.; Dragnea, V.; Tollin, G.; Zaleski, J. M.; Bauer, C. E. *Biochemistry* **2003**, *42*, 6726.
(39) Fukushima, Y.; Okajima, K.; Ikeuchi, M.; Itoh, S. *Photochem. Photobiol.* **2007**, *83*, 112.
(40) Domratcheva, T.; Grigorenko, B.; Schlichting, I.; Nemukhin, A. V. *Biophys. J.* **2008**, *94*, 3872.
(41) Stelling, A. L.; Ronayne, K.; Nappa, J.; Tonge, P.; Meech, S. *J. Am. Chem. Soc.* **2007**, *129*, 15556.
(42) Senn, H. M.; Thiel, W. *Top. Curr. Chem.* **2007**, *268*, 173.

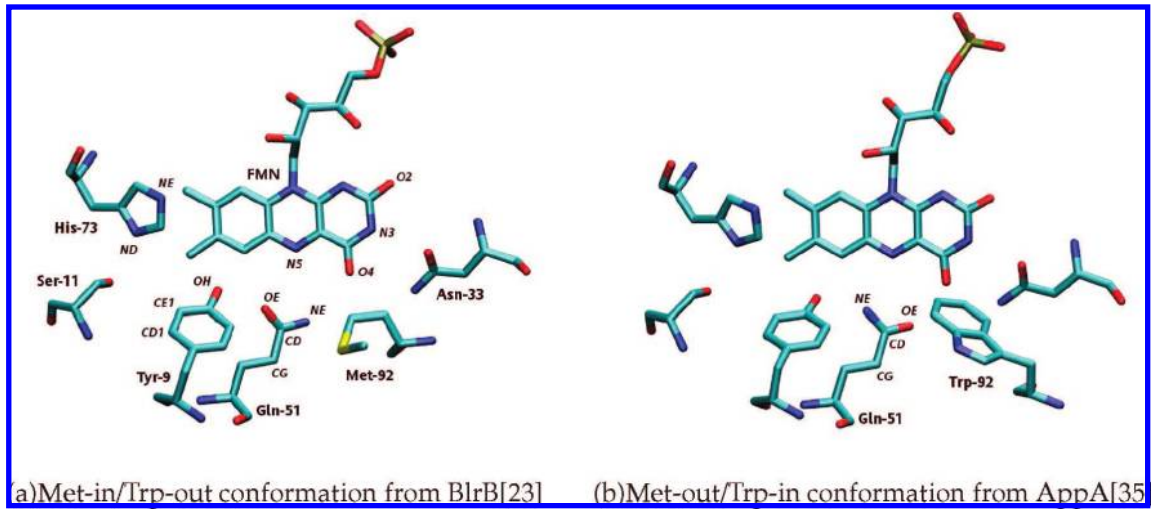


***Figure 2.*** Environment of flavin cofactor (FMN) in the different Met-in/Trp-out and Met-out/Trp-in conformations as found in the X-ray structures of BLUF domains. The terms Met-in and Trp-in are used in the following for the conformations shown in panels a and b, respectively.

Finally, the controversial role of Met-94 and Trp-92 residues (see Figure 2) for the signal transduction is investigated. Assuming that the signaling state (to which the observed 10 nm red-shift in absorption spectrum is assigned) is generated by tautomerization of the Gln moiety,[40,41] which is also one of the conclusions of the present work, the influence of protein conformations, differing in the position of Met-94 and Trp-92 residues, on the relative stability of Gln tautomer are considered. Calculations were carried out on the two Met-in (or Trp-out) and Met-out (or Trp-in) conformations, for which the terminology *Met-in* and *Trp-in* (see Figure 2, parts a and b) will be used throughout this paper. On the basis of the results obtained we conjecture that the Trp-in form corresponds to the final signaling state of BLUF domains.

## 2. Computational Details

The monomer A of the crystal structure of BlrB[23] (PDB code: 1BYC) was used to setup the QM/MM calculation. A pre-equilibrated water droplet (radius 20 Å) containing 5187 water molecules was used to solvate this initial structure. The droplet boundary of 2.5 Å was constrained with a quartic force of 0.2 [24 kcal/mol/Å$^2$] using the miscellaneous mean-field potential (MMFP). All bonds to hydrogen atoms were held by SHAKE.[43] For FAD we used the parameters available from CHARMM27 nucleic and amino acids[44−48] (see the Supporting Information). The system was heated from 50 to 300 K using a 1 fs time step and 10 K temperature increase for every 25th time step during which the backbone was constrained in a harmonic potential. This constraint was then lifted gradually, and the system was thereafter allowed to relax at 300 K over 500 000 time steps (≡ 500 ps). Simulations showed a large mobility of Tyr-9 next to Gln-51 and FAD (see the Results and Discussion section for further details). We found a buried pocket between Tyr-9 and Ser-11, which may be transiently occupied by a water molecule (denoted as WAT, see Figure 3) not observed in the X-ray structure analysis. Simulations with this additional buried water molecule stabilized the conformation of Tyr-9 in the same orientation as observed in the reference structure 1BYC. The input geometries for the QM/MM calculations were prepared by selecting representative structures from the molecular dynamics (MD) run and minimizing the selected structures using the force field.

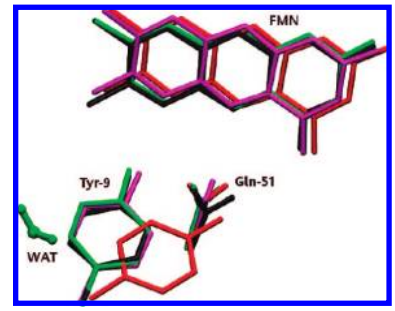


***Figure 3.*** Crystal structure of BlrB, shown in black, is superimposed on three configurations obtained from molecule dynamics simulations. The conformation shown in green corresponds to the case where an additional water molecule is placed within the cavity found near the Y9 residue. In the conformation shown in red, the Tyr-9 residue is severely dislocated relative to the crystal structure, whereas the conformation displayed in magenta coincides closely with the experimentally resolved structure. The MD simulations predict the magenta conformation as energetically more favorable than the red form.

The QM region naturally comprises FMN as the main chromophore and Tyr-9 since a CT process from Tyr-9 to FMN appears to play an essential role in the mechanism of the photocycle. Additionally, Gln-51 as a further key player, His-73 (protonated at NE, see Figure 2a), the WAT molecule, and its neighboring Ser-11 were also included in the QM region (see Figure 2a). The His-73 moiety, being rather close to FMN, might also be directly involved in the relevant excited states or at least significantly interact with FMN and Tyr-9 and therefore influence the energetic position of the CT state. Additionally, for calculating harmonic vibrational frequency and vertical excitation energy calculations at the proposed dark, intermediate, and signaling state structures, the above-mentioned QM region was augmented by Asn-33 and Trp-92. In order to explore the possible different pathways for biradical recombination a somewhat reduced QM region was employed, consisting of only FMN, Tyr-9, and Gln-51.

To study the possibility of Gln-51 tautomerization (imidate form of Gln-51) and the orientation exchange of the Trp-92 and the Met-94 residues (leading to the Trp-in and Met-in conformations, respectively) additional QM/MM calculation based on protein model

(43) Ryckaert, J.; Ciccotti, G.; Berendsen, H. *J. Comput. Phys.* **1977**, *23*, 327.
(44) MacKerell, A. D.; et al. *J. Phys. Chem. B* **1998**, *102*, 3586.
(45) Pavelites, J. J.; Gao, J. L.; Bash, P. A.; MacKerell, A. D. *J. Comput. Chem.* **1997**, *18*, 221.
(46) Foloppe, N.; MacKerell, A. D. *J. Comput. Chem.* **2000**, *21*, 86.
(47) MacKerell, A. D. J.; et al. *FASEB J.* **1992**, *6A*, 143.
(48) Brooks, B. R.; Bruccoleri, R. E.; Olafson, B. D.; States, D. J.; Swaminathan, S.; Karplus, M. *J. Comput. Chem.* **1983**, *4*, 187.

systems were carried out. To this end the wild-type BLUF−FAD complex and the imidate were created on the basis of the X-ray structure 1BYC. Due to the lack of any reliable Charmm parameters for the imidate tautomer of Gln-51 these models were initially minimized by using the force field MAB as implemented in the MOLOC program.[49,50] Thereafter, MD simulations of 10 ps were performed. A H-bond weight of 1.78 was applied, which corresponds to the H-bond strength parametrized for describing the intramolecular H-bond enthalpy rather than the intermolecular ligand binding H-bond free energy (default in MAB).

Furthermore, a second set of structures with a different orientation of the loop before $\beta$5 was generated. This loop includes the Trp-92 and Met-94 units. In the X-ray structure 1BYC the residue Met-94 is oriented toward Gln-51 next to FAD and Asn-33, whereas Trp-92 is exposed to the solvent (see Figure 2a). The second conformation with Trp-94 pointing in and Met-92 pointing outward toward the solvent was created by adopting the relevant environment of the X-ray structure 1YRX of the BLUF domain of AppA and 2HFN (chain D) of Slr1694 (see Figure 2b).

The QM/MM interface ChemShell[51] was used throughout in this study. The QM/MM coupling was calculated using the charge-shift scheme and link atoms.[51] For the MM part of the QM/MM calculations the DL_POLY molecular dynamics package[52] (with CHARMM force field parameters) was applied. The HDLCopt optimizer[53] implemented in ChemShell was employed for the QM/MM geometry optimizations, which has to be supplied with the incremental energy and the incremental nuclear energy gradient of the QM part. Geometry optimizations on the potential energy surface of the electronic ground state were carried out at the level of density functional theory (DFT) employing the B3LYP[54] hybrid functional and, for purpose of verification, also at the level of local Møller−Plesset perturbation theory of second order (LMP2).[55] For these energy functionals efficient analytic energy gradients are available.

Geometry optimizations on the potential energy surfaces of the electronically excited states, i.e., the CT surface (due to the lack of alternatives for extended systems of this size), were performed at the level of time-dependent DFT (TD-DFT) response theory, applying the analytical TD-DFT energy gradient program of Furche and Ahlrichs.[56] For that purpose the ChemShell interface had to be modified accordingly. It is well-known that TD-DFT grossly underestimates excitation energies of CT states (cf., ref 57 and references therein). This problem is directly related to the electronic self-interaction inherent in DFT[58,59] and can partly be alleviated by employing hybrid functionals with a larger fraction of Hartree−Fock exchange. The B3LYP functional (and naturally even more so the BP functional) turned out to dramatically underestimate the excitation energies of all kinds of CT states of the system (cf., Table 1), which in turn would mix with the LE state of interest. Therefore, instead of B3LYP the BHLYP functional[60] with a larger fraction of exact Hartree−Fock exchange was employed for the TD-DFT excited-state geometry optimizations. For individual TD-DFT optimized geometries the related excitation energies were also computed at the level of time-dependent coupled cluster response theory, utilizing the CC2 model.[61,62] This strategy of combining TD-DFT optimized geometries with CC2 response single-point excitation energy calculations was successfully employed by us recently in a study on the photophysics of a phenothiazine−phenylisoalloxazine dyad, where an electron-transfer process from phenothiazine to isoalloxazine is activated upon locally exciting the flavin chromophore.[57] The electronic ground-state calculations on the nonzwitterionic biradical along the different possible pathways of biradical recombination were carried out at the level of spin-unrestricted DFT. Here, in order to save computational resources, the B3LYP functional and the SVP basis set were used, which should do for that purpose.

***Table 1.*** Vertical Excitation Energies (in eV) Calculated at the TD-DFT and CC2 Levels of Theory for the Dark Structure (Y9-$\pi$/Q51-O$\varepsilon$)[a]

| character | BP | B3LYP | BHLYP | CC2 |
|---|---|---|---|---|
| LE(FMN) | 2.48 (0.110) | 2.81 (0.179) | 3.29 (0.269) | 2.99 (0.249) |
| CT(Y9 → FMN) | 0.88 (0.000) | 1.86 (0.000) | 3.17 (0.001) | 3.59 (0.000) |

[a] The oscillator strengths, *f*, are shown in parentheses.

For the (TD)-DFT and CC2 calculations, we used the TURBOMOLE[63] program package utilizing the def-TZVP[64] and cc-pVDZ basis sets, respectively. The local-MP2 calculations were performed with the MOLPRO[65] program employing the aug-cc-pVDZ[66] basis set.

## 3. Results and Discussion

**3.1. Search for a Representative Structure.** The first X-ray crystal structure of the dimer of the N-terminal AppA 17−133 BLUF domain was determined by Anderson et al.[35] and exhibits an $\alpha + \beta$ sandwich with the FAD aromatic moiety bound in between the two long helices of a ferredoxin-like fold. The dimer interface however is distorted by detergent molecules.

The NMR solution structure of the AppA BLUF domain was determined by Grinstead et al.[67] and shows essentially the same dimer structure as in the X-ray crystal structure, despite the fact that the orientation of the key Gln-51 residue and a C-terminal loop containing Trp-92 near flavin is not resolved. The structure of the light-induced signaling state of AppA BLUF domain is currently not known, but upon irradiation some residues show changes in the NMR chemical shifts, most of them located near or in the C-terminal region.[68] This dynamic behavior found in the NMR solution structure suggests that the C-terminal part of the BLUF domain is involved in the signaling and may sample different conformations.

Jung et al. also reported a crystal structure of mutated AppA 1−124 C20S BLUF domain in the dark state.[69] This structure shows a different orientation of the C-terminal stretch with a Met residue oriented toward Gln (see Figure 2a) and the Trp

(49) Gerber, P. R. *J. Comput.-Aided Mol. Des.* **1998**, *12*, 37.
(50) Gerber, P. R.; Muller, K. *J. Comput.-Aided. Mol. Des.* **1995**, *9* (3), 251.
(51) Sherwood, P.; et al. *J. Mol. Struct. (THEOCHEM)* **2003**, *1*, 632.
(52) Smith, W.; Yong, C.; Rodger, P. *Mol. Simul.* **2002**, *28*, 385.
(53) Billeter, S. R.; Turner, A. J.; Thiel, W. *Phys. Chem. Chem. Phys.* **2002**, *2*, 2177.
(54) Becke, A. D. *J. Chem. Phys.* **1993**, *98*, 5648.
(55) Schütz, M.; Werner, H.-J.; Lindh, R.; Manby, F. R. *J. Chem. Phys.* **2004**, *121*, 737.
(56) Furche, F.; Ahlrichs, R. *J. Chem. Phys.* **2002**, *117*, 7433.
(57) Sadeghian, K.; Schütz, M. *J. Am. Chem. Soc.* **2007**, *129*, 4068.
(58) Dreuw, A.; Weisman, J. L.; Head-Gordon, M. *J. Chem. Phys.* **2003**, *119*, 2943.
(59) Tozer, D. *J. Chem. Phys.* **2003**, *119*, 12697.
(60) Becke, A. D. *J. Chem. Phys.* **1993**, *98*, 1372.
(61) Christiansen, O.; Koch, H.; Jørgensen, P. *Chem. Phys. Lett.* **1995**, *243*, 409.
(62) Hättig, C.; Weigend, F. *J. Chem. Phys.* **2000**, *113*, 5154.
(63) Ahlrichs, R.; Bär, M.; Horn, H.; Kömel, C. *Chem. Phys. Lett.* **1989**, *162*, 165.
(64) Schäfer, A C. H.; Ahlrichs, R. *J. Chem. Phys.* **1994**, *100*, 5829.
(65) Werner, H.-J.; Knowles, P. J.; Lindh, R.; Manby, F.; Schütz, M.; et al. *MOLPRO, a Package of ab Initio Programs*, version 2006.2, 2006; see http://www.molpro.net.
(66) Kendall, R. A.; Dunning, T. H.; Harrison, R. J. *J. Chem. Phys.* **1992**, *96*, 6796.
(67) Grinstead, J. S.; Hsu, S. T.; Laan, W.; Bonvin, J. J. M. A.; Hellingwerf, K. J.; Boelens, R.; Kapstein, R. *ChemBioChem* **2006**, *7*, 187.
(68) Grinstead, J. S.; Avila-Perez, M.; Hellingwerf, K. L.; Boelens, R.; Kapstein, R. *J. Am. Chem. Soc.* **2006**, *128*, 15066.
(69) Jung, A.; Reinstein, J.; Domratcheva, T.; Shoeman, R. L.; Schlichting, I. *J. Mol. Biol.* **2006**, *362*, 717.

residue pointing out to the solvent. Similar orientations for the Trp and Met residues are observed in the crystal structures of BlrB,[23] Tll0078,[29] and Slr1694.[25,70] In the following we will denote such conformations as *Met-in*, whereas for the crystal structure proposed by Anderson et al.[35] the term *Trp-in* will be used (see Figure 2b).

The orientation of the Gln-51 moiety in the dark state has also been the subject of some debate. In the Met-in crystal structures the amide group of Gln-51 acts as a hydrogen-bond donor to the FMN-N5, whereas the C═O group is the acceptor of a hydrogen bond from Tyr-9-OH (see Figure 2a). In the Trp-in structures, on the other hand, the carbonyl group of Gln-51 is rotated about the CG−CD bond by 180° as shown in Figure 2b. As a structural basis for our theoretical study we adopted the high-resolution dark-state structure of the well-characterized BlrB BLUF protein solved by Jung et al.[23]

Of primary interest in the present context are the photoinduced processes involved in the formation of the signaling state, taking place in the active site of the BLUF domains in the vicinity of the FMN cofactor. Since this active part of the protein shows a strong conformational similarity for all structurally known BLUF domains and furthermore the structural rearrangements are small on going from the dark/receptor to the light/signaling state (as apparent from the small 10 nm shift in the absorption spectrum), it appears to be sufficient to consider one representative structure.

In our initial MD simulations a significant instability in the orientation of the Tyr-9 moiety relative to the flavin cofactor was observed (cf., Figure 3). The Tyr-9 residue appears to switch between two distinct orientations (colored red and magenta in Figure 3). This switching motion is modulating the interaction of the environment with the FMN chromophore. The energetic position of the CT state is anticipated to be very sensitive to the environment, certainly much more so than the LE state carrying the oscillator strength. Therefore, the relative energetic position of LE and CT state, a key property for the conjectured mechanism, is expected to differ appreciably for the two orientations of Tyr-9. However, only one of the two orientations is in good agreement with all published crystal structures to this date for the BLUF domains; in the other conformation the TYR ring is severely dislocated relative to the crystal structure.

As already pointed out in the previous section an additional water molecule (WAT) was placed into the cavity of the crystal structure between the Tyr-9, His-73, and Ser-11. This was motivated by the fact that the isotropic displacement (B-factor) of the phenyl ring of Tyr-9 is asymmetric and the atoms CD1 and CE1 (shown in Figure 2a) oriented toward Ser-11 show a higher mobility. The MD run performed for the BlrB BLUF domain in the presence of WAT, which is primarily interacting with Tyr-9, exhibits a much more stable orientation of this amino acid leading to conformations in close agreement with the known crystal structures.

Two different types of H-bond interactions between WAT and Tyr-9 were observed, where in both cases WAT acts as the H-bond donor and the Tyr-9 ring or the Tyr-9 oxygen atom as the corresponding acceptor. We employ the notation Y9-$\pi$ and Y9-OH for these two orientations, respectively (see Figure 4, parts a and b).

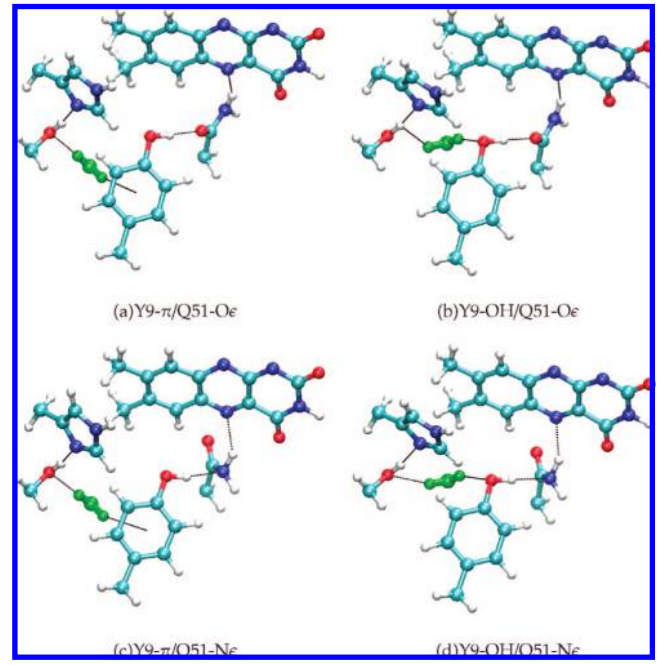


***Figure 4.*** Comparison of the ground-state structures obtained by MD minimizations. The water molecule (WAT) is a H-bond donor to the ring (Y9-$\pi$) or to oxygen atom (Y9-OH) of the Tyr-9 amino acid. The Gln-51 (Q51) is the H-bond acceptor, either through the carbonyl group (Q51-O$\varepsilon$) or the amine group (Q51-N$\varepsilon$).

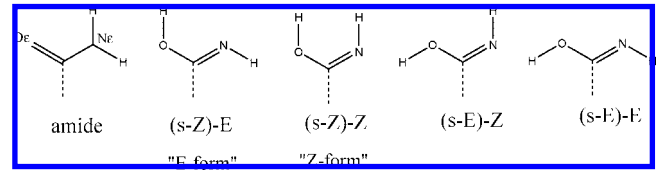


***Figure 5.*** Different tautomer/isomers of Gln, nomenclature taken from ref 71.

The orientation of the Gln-51 is a further issue: in the crystal structure of BlrB the orientation of Gln-51 is such that the carbonyl group of Gln-51 and the OH group of Tyr-9 form a H-bond. The label Q51-O$\varepsilon$ (the O$\varepsilon$ and N$\varepsilon$ atoms of Gln are shown in Figure 5) is used in the following to denote such an orientation, thereby emphasizing the role of C═O as the H-bond acceptor in this alignment. The MD simulations do not reveal any tendency for an orientation of Gln-51 different to Q51-O$\varepsilon$. This actually also holds true for MD simulations in absence of WAT. This is not unexpected due to the rigidity of the environment around Gln-51 which prevents a rotation of Gln-51 even for the case of a much more fluxional Tyr-9 orientation, i.e., without WAT. Nevertheless, orientations of Gln-51 different to Q51-O$\varepsilon$ are frequently discussed in the literature.[32,35,67,68] Therefore, alternative orientations of Gln-51, generated by systematic rotation of the amide group of this residue, were studied in the context of this work. Our attempts to find a minimum structure which would correspond to a 180° flipped Gln-51 residue (as shown in Figure 2b) failed. Instead a rather stable arrangement was found where the Gln carbonyl group is pointing away from the Tyr-9 residue which corresponds to a rotation of roughly 90° about the CG−CD bond of Gln-51. The former still acts as H-bond donor, namely, to the Gln-N$\varepsilon$ (see Figure 4, parts c and d). For these possible conformations the notation Q51-N$\varepsilon$ is used in the following.

(70) Only in one monomer (D) of Slr1694 we find the Trp-92 inside the protein and next to Gln-51; however, there seems to be no H-bond interaction between these two residues.

(71) Duvernay, F.; Chatron-Michaud, P.; Borget, F.; Birney, D.; Chiavassa, T. *Phys. Chem. Chem. Phys.* **2007**, *9*, 1099.

***Table 2.*** Relative Ground-State Energies (in kcal/mol) of the QM/MM Minimum Energy Structures Obtained by LMP2/Charmm and DFT/B3LYP/Charmm, Respectively[a]

| structure | LMP2/Charmm | B3LYP/Charmm |
|---|---|---|
| Y9-$\pi$/Q51-O$\varepsilon$ | 0.00 | 0.00 |
| Y9-OH/Q51-O$\varepsilon$ | 3.65 | 10.84 |
| Y9-$\pi$/Q51-N$\varepsilon$ | 3.54 | 2.25 |
| Y9-OH/Q51-N$\varepsilon$ | 9.13 | 16.81 |

[a] The QM/MM ground-state energy of the Y9-$\pi$/Q51-O$\varepsilon$ structure is taken as reference.

The four geometries displayed in Figure 4 represent the four possible orientations of WAT and Gln-51 relative to the Tyr-9 residue, respectively. The orientations of all the other amino acids in the vicinity of flavin, which are highly conserved in various BLUF domains, remain very similar to those of the crystal structure during the MD simulation runs. After equilibration the four individual geometries of Figure 4 were optimized by using the force field in order to get good starting geometries for the subsequent QM/MM optimizations.

**3.2. Ground-State QM/MM: Determination of the Most Stable Dark-State Structure.** The QM/MM geometry optimizations were carried out by applying LMP2 or DFT/B3LYP for the QM part in combination with the Charmm force field for the MM part (vide infra). The results are compiled in Table 2. The most stable geometry clearly corresponds to the Y9-$\pi$/Q51-O$\varepsilon$ arrangement. The alternative Y9-$\pi$/Q51-N$\varepsilon$ structure with the Gln-51 carbonyl group being rotated by $\approx$90° relative to the experimental crystal structure of BlrB is about 3.5 kcal/mol (LMP2) or 2.3 kcal/mol (DFT/B3LYP) less stable and most likely not a viable candidate for the dark-state structure. Furthermore, a preference for WAT to form a H-bond to the Tyr-9 ring (Y9-$\pi$ structures) rather than to the oxygen atom of Tyr-9 (Y9-OH structures) is observed. Such hydrogen bonds also occur in the electronic ground state of 2-naphthol clustered with two water molecules.[72] On the basis of these results we postulate that Y9-$\pi$/Q51-O$\varepsilon$ indeed represents the dark-state (receptor state) structure from which photoinduced processes are triggered. Consequently, all further calculations presented here use Y9-$\pi$/Q51-O$\varepsilon$ as their starting point.

**3.3. Choice of QM Method for the Excited States.** Vertical excitation energies and oscillator strengths for the relevant LE and CT states were calculated with TD-DFT and CC2 response theory at the Y9-$\pi$/Q51-O$\varepsilon$ DFT/B3LYP geometry. The resulting values are compiled in Table 1. Related differential densities between ground- and excited-state densities were also computed with TD-DFT/BHLYP and plotted in Figure 6. For reasons outlined in section 2, we consider TD-DFT results calculated with the BP or B3LYP functionals as entirely untrustworthy. The largest oscillator strength of 0.269 (TD-DFT/BHLYP) and 0.249 (CC2) was obtained for the LE state of flavin, which must correspond to the experimentally measured absorption bands around 450 nm (2.75 eV). It is evident from Figure 6 that the differential density of the LE excitation is entirely localized on the isoalloxazine subunit. CC2 response is overestimating the experimental value for the excitation energy by about 0.25 eV, as expected for this method/basis, whereas TD-DFT/BHLYP is overestimating it by 0.54 eV. The lowest CT state involves transfer of an electron from Tyr-9 to FMN, as is evident from Figure 6. According to the CC2 reference calculations, it lies energetically *above* the LE state for the Y9-$\pi$/Q51-O$\varepsilon$ geometry and carries virtually no oscillator strength. This is very similar to the situation encountered in a phenothiazine−phenyl-isoalloxazine dyad studied by us previously, where the CT state responsible for fluorescence quenching is populated via the LE state through a conical intersection.[57] For the present system we hence postulate an analogous mechanism to populate the CT state which is corresponding here to a zwitterionic biradical involving the partially positively charged Tyr-9 and the partially negatively charged isoalloxazine subunits, respectively. This hypothesis is supported experimentally by the low fluorescence quantum yield and the short lifetime of the excited FMN measured in BLUF domains.[21,22,24,28,32]

The TD-DFT/BHLYP method does not provide the correct ordering of LE and CT state and is therefore not able to predict or locate such a conical intersection (in contrast to CC2 response). On the other hand, the TD-DFT/BHLYP excitation energy of the CT state is not nearly as low and wrong as it is for the other two functionals. More importantly, the character and oscillator strength of the LE state provided by TD-DFT/BHLYP closely resembles that provided by CC2 for all relevant geometries, which turns out not to be the case for the other two functionals. Therefore, TD-DFT/BHLYP was used for all excited-state geometry optimizations including those on the CT surface.

**3.4. Charge-Transfer QM/MM: Biradical Formation Mechanism.** By exploring the CT surface in the vicinity of the Y9-$\pi$/Q51-O$\varepsilon$ ground-state minimum geometry it turned out that along the coordinate of proton transfer from Tyr-9 to Gln-51, labeled as $P_1$ in Figure 7, the total energy of the CT state is decreasing steeply. A sequence of constrained geometry optimizations along this pathway was then performed. The difference of the distance between H and the oxygen atoms of Tyr-9 and Gln-51, respectively (denoted by $\Delta_1$, cf., Figure 7), was defined as the constraint. All other degrees of freedom were fully relaxed. On going from the geometry corresponding to $\Delta_1 = -0.5$ (proton still on the side of Tyr-9 $\approx$ $Y9^{\bullet+}-Q51-FMN^{\bullet-}$ structure) to that corresponding to $\Delta_1 = +1$ (proton transferred to Gln-51 $\approx$ $Y9^{\bullet}-Q51^{+}-FMN^{\bullet-}$ structure) the CT state drops in energy by 6 kcal/mol (total QM/MM energy of the CT state). The excitation energy alone decreases at the same time from 0.99 to 0.1 eV (TD-DFT, BHLYP) or from 1.41 to 0.31 eV (CC2). This is a clear indication that after the postulated population of the CT state (via LE by conical intersection) the CT state relaxation proceeds via proton transfer ($P_1$) from Tyr-9 to Gln-51. A full geometry optimization (without constraints) on the CT state surface starting from Y9-$\pi$/Q51-O$\varepsilon$ directly leads to a structure where the proton is fully transferred to Gln-51, implying that this proton transfer proceeds without any barrier in between.

An efficient and accurate way to locate the extremal points on the conical intersection seam requires analytical gradients of the individual excited states and their nonadiabatic coupling vector (cf., ref 74 and references therein). For the current system the analytical energy gradients at the CC2 level of theory are clearly too expensive. An alternative strategy used previously for the phenothiazine−phenyl-isoalloxazine dyad[57] involves a combination of TD-DFT geometry optimization and CC2 single-point calculations. With the use of this approach minimum energy structures on the conical intersection seam can be roughly determined. However, this is a rather tedious procedure requiring

(72) Schemmel, D.; Schütz, M. *J. Chem. Phys.* **2008**, *129*, 034301.
(73) Humphrey, W.; Dalke, A.; Schulten, K. *J. Mol. Graphics* **1996**, *14*, 33–38.
(74) Sicilia, F.; Blancafort, L.; Bearpark, M.; Robb, M. *J. Chem. Theory Comput.* **2008**, *4*, 257.

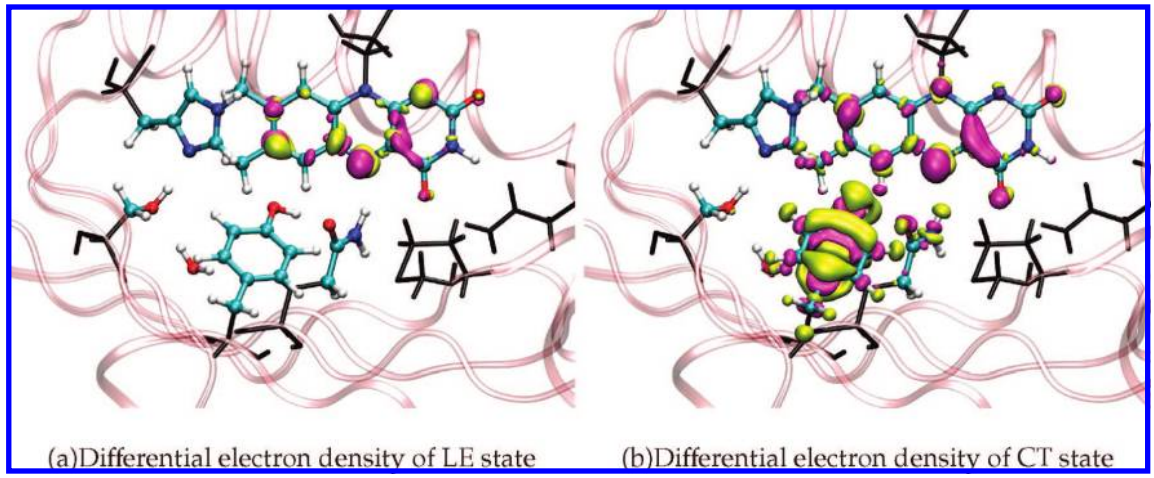


***Figure 6.*** Difference in ground and excited electron densities upon excitation. Yellow and magenta regions represent regions with loss and gain of electron density, respectively. All the graphics presented here have been prepared by the VMD package (ref 73).

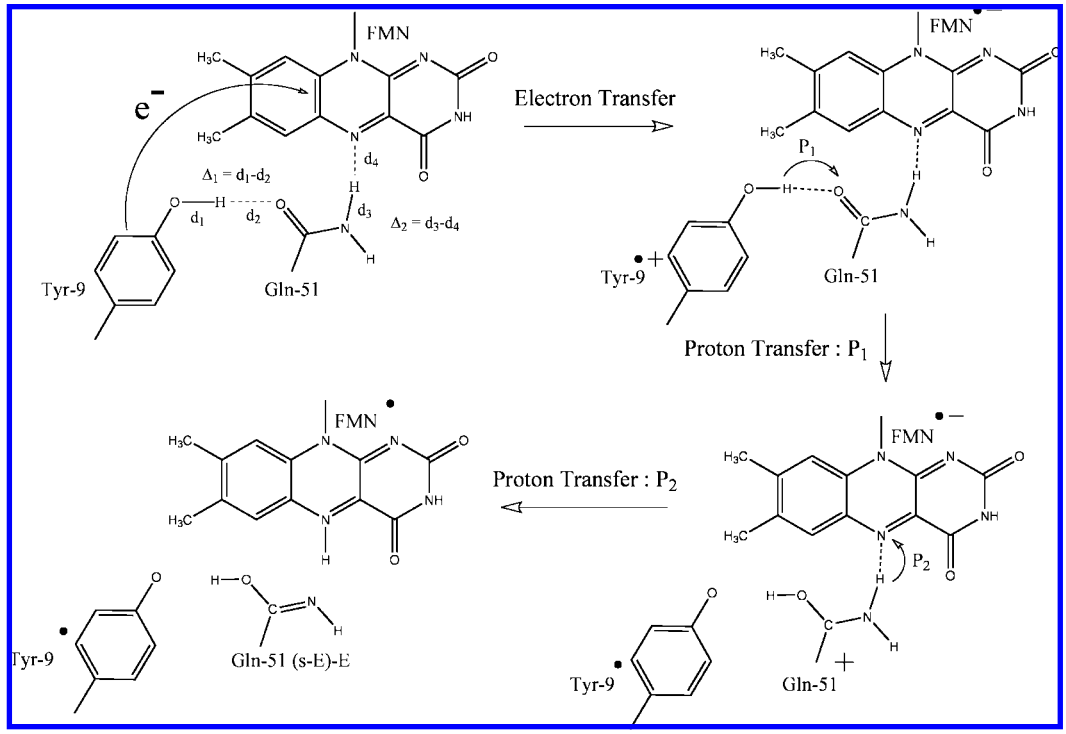


***Figure 7.*** Y9•−Q51−FMN• biradical formation path.

a very large number of calculations, and we have therefore decided not to pursue this issue in the present work.

Nevertheless there is strong evidence that the conical intersection indeed exists: when the Y9-$\pi$/Q51-O$\varepsilon$ and $\Delta_1 = -0.5$ structures are compared, the sole appreciable structural change in the flavin binding pocket is the slight displacement of the Tyr-9 proton. One may therefore consider the $\Delta_1 = -0.5$ structure to be very close to the Franck−Condon (Y9-$\pi$/Q51-O$\varepsilon$) structure. Yet the CT excitation energy has dropped dramatically, from 3.59 eV (dark) to 0.99 eV ($\Delta_1 = -0.5$) and is energetically already *below* the LE state at the latter geometry. This implies that the Franck−Condon point is located rather close to the conical intersection seam between these two states.

In the process of the first proton transfer ($P_1$), the distance between FMN-N5 and the closest hydrogen of the Gln-51 amino group is shrinking from 2.15 Å at the Franck−Condon point (Y9-$\pi$/Q51-O$\varepsilon$) to 1.83 Å at the $\Delta_1 = +1$ geometry. This indicates that the next consecutive step in the relaxation process on the CT surface is a second proton transfer from the Gln-51 amino group to FMN-N5, labeled as $P_2$ in Figure 7, leading to the Y9•−Q51−FMN• biradical where the charge separation induced by photoexcitation, i.e., the zwitterionic character, is equalized (cf., Figure 7). At the Y9•−Q51$^+$−FMN•$^-$ geometry the CT excitation energy is already very low, 0.1 eV (TD-DFT, BHLYP) or 0.31 eV (CC2), and it continues to decrease along the second proton transfer coordinate ($P_2$) in such a manner that a second conical intersection seam between CT and ground-state surface is crossed. The closed-shell DFT/BHLYP ground state becomes variationally instable after a certain point along the coordinate is passed, and the biradical is taking over the role of the electronic ground state. Time-dependent response methods like TD-DFT or coupled cluster response theory rely

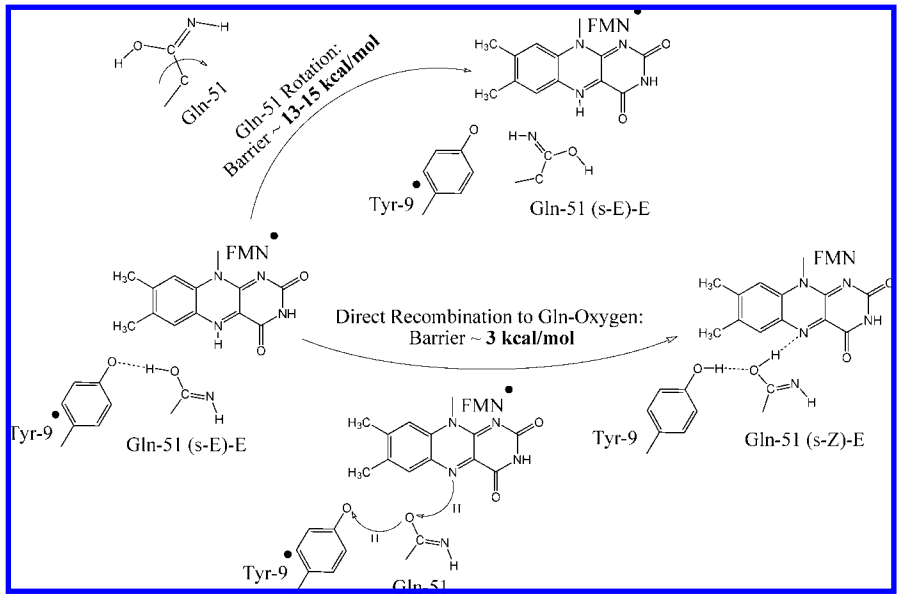


***Figure 8.*** Our proposed radical recombination to the oxygen of Gln-51 vs rotation of Gln-51 in the biradical Y9•−Q51−FMN• state prior to radical recombination.

on a closed-shell reference wave function for the ground state; hence, any conical intersection between the electronic ground state and an excited state cannot be dealt with (instead, multireference methods with appropriate active spaces would have to be utilized, which, however, are very cumbersome to use in such extended systems). Hence, no attempt was made to exactly locate the point where the proton transfer pathway dissects the conical intersection seam. The final Y9•−Q51−FMN• biradical form was generated by placing the second proton (of Gln-51) at distance of ≈1 Å and fully relaxing this structure thereafter by employing spin-unrestricted DFT/B3LYP. Of course the resulting wave function describing the biradical is no longer a pure singlet state; at the Y9•−Q51−FMN• geometry an eigenvalue of $S^2$ of 1.05 was obtained, as anticipated for a biradical described by a spin-unrestricted single determinant.

These results all indicate that the CT state, once activated via conical intersection with the LE state, opens a downhill channel within which the first and second proton transfer processes (from Tyr-9 to FMN, via Gln-51) occur without any barrier and finally lead to the formation of the nonzwitterionic biradical Y9•−Q51−FMN• species. As is evident from Figure 7 the process of generating the Y9•−Q51−FMN• species involves the tautomeriztion of the Gln-51 to the imidic form (amide → (*s*-*E*)-*E*, nomenclature taken from ref 71; see Figure 5) without rotation.

**3.5. Open-Shell QM/MM: Biradical Recombination Path. 3.5.1. Biradical Recombination via Gln-51 Rotation.** According to the experiments, the Y9•−Q51−FMN• biradical form has a lifetime of 65 ps[32] after which the biradical recombination step is completed. Any proposed process which leads to the loss of the biradical signal must therefore be compatible with a lifetime of this order of magnitude. In order to examine the possibility of Gln rotation as suggested by Domratcheva et al.,[40] we carried out a series of constrained geometry optimizations of the neutral biradical state along the rotation angle about the C−C bond of Gln-51 (see Figure 8). These calculations were again performed by applying spin-unrestricted DFT with the B3LYP functional. Our results indicate that, depending on the direction of rotation, a barrier of 13−15 kcal/mol has be to be surmounted. This high barrier implies a lifetime of the Y9•−Q51−FMN• biradical form of several milliseconds instead of the 65 ps imposed by the experiment. In our view, two major factors contribute to this barrier, which is by far too high to be overcome within nanoseconds upon excitation: (i) There is a strong H-bond, namely, Tyr-9-O•/Gln-51-OH, and a weak interaction between Met-94-S and Gln-51-$NH_2$ which needs to be cleaved during the process of rotation. (ii) There are four amino acids around the Gln-51 residue, namely, Leu-42, Ile-53, Ile-67, and Met-94, which are highly conserved and block rotation of Gln-51 via steric hindrance. For the complete conservation pattern of the BLUF family see the Supporting Information. Moreover, there are additional rotations required (about the NH double and OH single bonds of Gln-51) in order to get the particular geometry, which, according to Domratcheva et al., is finally enabling biradical recombination. Appreciating all this, it appears as unlikely that the radical recombination proceeds via rotation of Gln-51.

**3.5.2. Biradical Recombination without Gln-51 Rotation.** An alternative to the rotation of Gln-51 is the formation of the imidic form of Gln-51 ((*s*-*Z*)-*E* form). We postulate that the hydrogen atom on FMN-N5 is transferred to the Gln-51 oxygen directly. Our calculations predict a barrier of about 3 kcal/mol for such a process (Figure 8) which involves the isomerization ((*s*-*E*)-*E* → (*s*-*Z*)-*E*; these isomers are shown in Figure 5) of Gln-51. This barrier indeed matches nicely with the experimental lifetime of 65 ps of the biradical state (vide supra). Moreover, a much smaller distortion in the conformation of the protein as a whole, namely, a small change in the alignment of the hydrogen donor/acceptor groups (i.e., from FMN-N5/Q51-N$\varepsilon$ to FMN-N5/Q51-O$\varepsilon$) is sufficient to allow this step for taking place. When the aforementioned barriers are compared, we conjecture that the rotation of the Gln-51 moiety is not a competitive step and therefore unlikely to be of relevance for the mechanism of signaling state formation.

**3.6. Path to the Signaling State.** As pointed out in the Introduction the red-shift of the IR absorption band assigned to the stretch mode of the C4═O4 bond is anticipated to be caused by the formation of a new hydrogen bond at the O4 position of

FMN. Such a hydrogen bond was postulated to be formed after the rotation of the Gln-51 residue.[16,32,34,40,75,76] So far we have shown that the structure with Gln-51 in its (*s-Z*)-*E* form, denoted as Q51-*E*, which is immediately reached upon recombination does not involve any rotation of Gln-51. In the geometry Q51-*E*, however, no new H-bond to FMN-O4 can be formed. Therefore, alternative imidic forms of Gln-51 were considered, for which such a H-bond is possible. Due to the high barrier of Gln-51 rotation a viable alternative is the *Z*-form of Gln-51 (see Figure 5). The latter conserves the H-bond between its OH group and FMN-N5, which is also present in the Q51-*E* geometry. QM/MM geometry optimizations (employing the very same QM/MM specifications as before) on conformations containing the *E*- and *Z*-forms of the Gln-51 moiety reveal that the *E*-form of Gln-51 is preferred over the *Z*-form, in spite of the additional H-bond. It appears that the *Z*-form of Gln-51 is destabilized by the neighboring Met-92 due to repulsion between the sulfur atom of Met-92 and the lone pair of the NH group of Gln-51.

At first glance it may seem as if the Q51-*E* structure contradicts experimental findings, since the expected H-bonding interaction is missing. There is, however, evidence for a fast transforming intermediate in AppA, BlrB,[69] and Tll0078,[30] which can be only trapped at low temperatures. The measured shift of the LE band in the UV−vis spectrum for this intermediate amounts to about half of that measured for the final signaling state. Fukushima et al., for example, report about a 5 nm red-shifted intermediate for the BLUF domain of Tll0078.[30] These authors conclude that further conformational changes in the protein environment in the vicinity of FMN are necessary to arrive at the signaling state with its characteristic 10 nm red-shift feature. A similar conclusion was made by Jung et al. for intermediates detected in AppA and BlrB BLUF domains.[69] Taking into account that biradical formation (via the proton transfer processes driven by the CT state) and the subsequent *fast* biradical recombination steps studied in the present work involve movement of only light hydrogen atoms/protons and therefore are feasible in crystalline structures or low temperatures, we assign the Q51-*E* structure to the observed intermediate on the path toward the final signaling structure.

As mentioned in the Introduction the position/orientation of the Trp-92 residue with respect to FMN is not well-defined in both dark- and signaling state conformations. One may therefore assume that this residue may well be involved in the aforementioned conformational changes upon receptor ↔ signaling state transitions. In the FT-IR study carried out by Masuda et al.[77] the mutation of the Trp-92 residue in AppA BLUF domain was shown to weaken the hydrogen-bonding network around FMN-O4, although the overall dark → light red-shift for the C4═O4 IR mode was not affected. Additionally, this mutation leads to a dramatic increase in the rate of thermal relaxation toward the dark state.[77] The presence of Trp-92 in BLUF domains therefore seems to stabilize the signaling state conformation. Hence it is of interest to compare the *E*- and *Z*-forms of the Gln-51 moiety for a Trp-in conformation.

Unfortunately, there is no crystal structure available for a possible Trp-in conformation of the BLUF domain of BlrB. On the basis of Trp-in conformations published for AppA[35] and Slr1694[25] we made a model system for a possible Trp-in conformation for BlrB, which then was used as the starting structure for further QM/MM calculations (see section 2 for details about the preparation of this model system). In contrast to the Met-in case, the *Z*-form of Gln-51 now is more stable than the *E*-form for the Trp-in model of the protein. This result now also provides an explanation for the much faster dark-state recovery of the Trp-92 mutant, since the additional stabilization of the H-bond network around FMN-O4, caused by the latter residue, is missing in the mutant. The Trp-in conformation with Gln-51 in its (*s-Z*)-*Z* form is denoted as Q51-*Z*.

The transition from the Met-in Q51-*E* to the Trp-in Q51-*Z* geometry involves a further isomerization step ((s-*Z*)-*E* → (s-*Z*)-*Z*, cf., Figure 5, or *E* → *Z* for short) of the Gln-51, which corresponds to inversion of the N−H bond. An alternative would be the thermal back-reaction to the original dark-state conformation via (*s-Z*)-*E* → amide tautomerization. In order to estimate the barriers for the mentioned tautomerization and isomerization processes, gas-phase calculations (DFT/B3LYP employing the TZVP basis) for the Gln-51 model systems (as shown in Figure 5) were performed. A barrier of about 33 kcal/mol for the imidic (*s-Z*)-*E* → amide tautomerization was obtained, whereas for the *E* → *Z* isomerization step the barrier is about 28 kcal/mol. Additional water molecules, which enable a concerted proton transfer, reduce the barrier further to 22 kcal/mol as additional test calculations have shown.

Having three representative QM/MM optimized structures, dark, Q51-*E*, and Q51-*Z* at hand, the next step is to include the Asn-33 and Trp-92 residues in the QM region. Experimentally, these have been shown to influence both UV−vis spectra and IR spectra, as well as the signaling → dark-state transition rate, as mentioned earlier. Therefore they need to be included at the more accurate QM level for the vertical excitation and vibrational frequency QM/MM calculations (see below). For the dark and Q51-*E* geometries the initial QM region (set A) was augmented by Asn-33 (set B). For the Q51-*Z* geometry set A was augmented by Asn-33 and Trp-92 (set C), respectively. The following observations, made by comparing the QM/MM optimized structures shown in Figure 9, are complementary to the further QM/MM results discussed in subsections 3.7 and 3.8 dealing with the vertical excitation energy and vibrational frequency calculations performed for the above-mentioned three structures.

It is, for example, evident that the rather weak $NH_2$−N5 H-bond at the dark geometry, is replaced by a stronger OH−N5 H-bond (at the Q51-*E* geometry) after the direct biradical recombination process discussed above. On going from the Q51-*E* to the Q51-*Z* structure the length of this OH−N5 H-bond between FMN and Gln-51 remains virtually constant. Recalling that the electron density of the LE state increases considerably at the N5 position of flavin (see Figure 6a), this former observation is a clear indication that the H-bond at N5 position, which we expect to be partially responsible for the slight red-shift of the band related to the LE state, as observed in the UV−vis spectrum, is not disturbed by even the rather large conformational change of the Trp−Met flip. This is in agreement with the flash-photolysis experiment carried out by Gauden et al.[78] where the authors conclude that the red-shifted absorption

(75) Unno, M.; Masuda, S.; Ono, T.-A.; Yamauchi, S. *J. Am. Chem. Soc.* **2006**, *128*, 5638.
(76) Toh, K.; van Stokuum, I.; Hendriks, K.; Alexandre, M. T.; Arents, J. C.; Perez, M.; van Grondelle, R.; Hellingwerf, K.; Kennis, J. T. *Biophys. J.* **2008**, *95*, 312.
(77) Masuda, S.; Hasegawa, K.; Ono, T.-A. *Plant Cell Physiol.* **2005**, *46*, 1894.
(78) Gauden, M.; Yeremenko, S.; Laan, W.; van Stokkum, I. H. M.; Ihalainen, J. A.; van Grondelle, R.; Hellingwerf, K. J.; Kennis, J. T. M. *Biochemistry* **2005**, *44*, 3653.

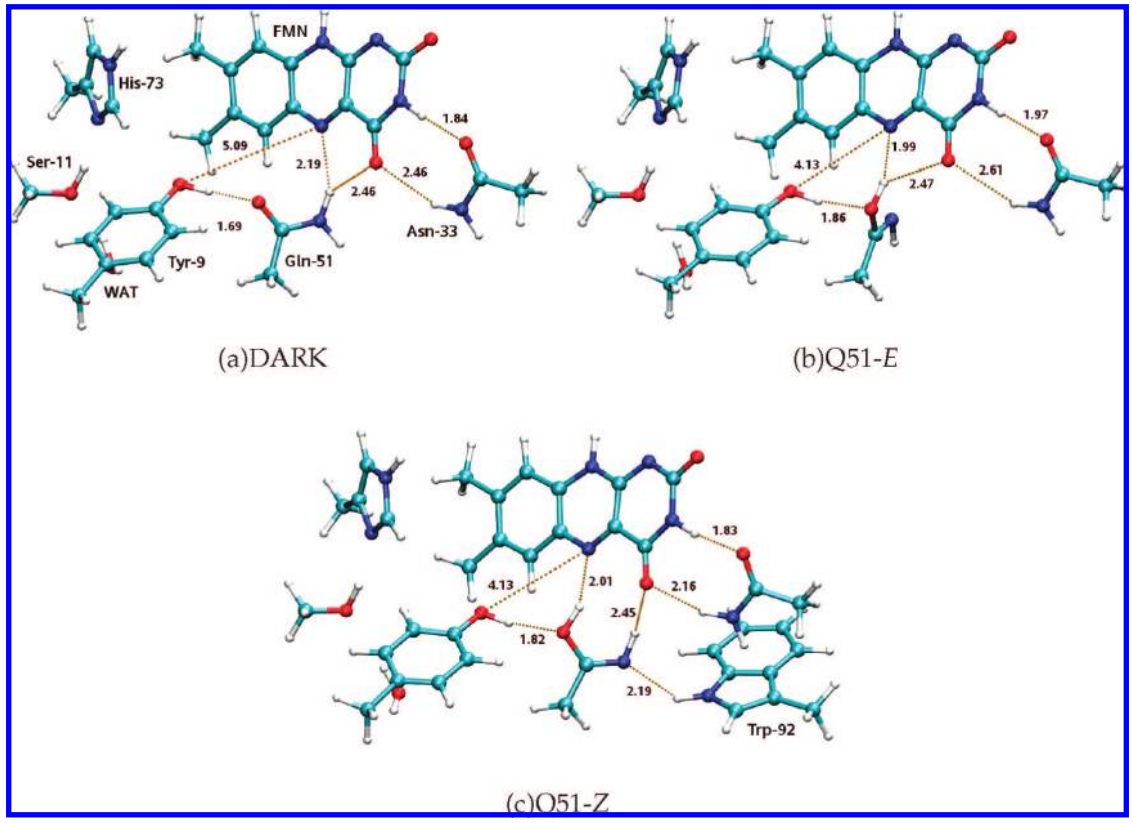


***Figure 9.*** Optimized ground-state QM/MM structures for the dark, Q51-*E*, and Q51-*Z* conformations.

band of the signaling state appearing after less than 10 ns after initial excitation of the dark structure does not change thereafter within the observed time range of 10 ns to some milliseconds.

Another strong H-bonding interaction between Asn-33 and FMN-O4 is formed during the signaling state formation as can be seen by comparing the dark and Q51-*Z* (our proposed dark and signaling state) conformations (Asn-33-H/FMN-O4 distance: 2.46 vs 2.16 Å, see Figure 9, parts a and c). This is in line with crystal structures solved for BLUF domains corresponding to Trp-in conformations. Considering the slight increase in the electron density at the FMN-O4 position after excitation to the LE state, the stronger H-bond formed between FMN-O4 and Asn-33 could be of importance for inducing the red-shift observed in the UV−vis absorption spectrum. In fact, Asn-33 mutated BLUF domains show only half of the red-shift observed for the wild type,[29] which is in agreement with the role proposed here for this residue.

This strengthened hydrogen-bonding interaction between FMN-O4 and Asn-33 could also be the main reason for the red-shift in the IR vibrational C4═O4 stretch mode of FMN. There is a second H-bond between the *Z*-tautomer of Gln-51 and FMN-O4, only found after inversion of the N−H bond (discussed above), yet one expects the stronger H-bond (Asn-33/FMN-O4, Figure 9c) to be *the* hydrogen bond formed during the signaling state formation hence causing the red-shift in the C4═O4 stretch mode.

**3.7. Vertical Excitation Energies: Comparison of Dark, Q51-*E*, and Q51-*Z* Structures.** Vertical excitation energies at the dark, Q51-*E*, and Q51-*Z* geometries were computed by applying both TD-DFT (using the B3LYP and BHLYP functionals) and CC2 response theory. It has been stated already above that we do not consider the TD-DFT (B3LYP) values as reliable, certainly not for the CT state; they are just given here for comparison. The QM/MM regions were specified as the sets A, B, and C (vide supra), respectively, and the results so obtained are compiled in Table 3.

**3.7.1. Locally Excited State (FMN → FMN*).** No substantial differences in the excitation energies of the LE state are apparent between the individual geometries. Red-shifts of 0.07 eV (9.8 nm) and 0.1 eV (15.0 nm) between the excitation energies of the dark and Q51-*Z* geometries were obtained at the level of CC2 response theory for the QM regions A and B/C, respectively. This is basically in agreement with experiment since all known BLUF domains do not feature any substantial spectral shift of the LE absorption band between dark and signaling state. The good agreement of our values above with the experimental red-shift of 10 nm must be considered as fortuitous. A shift of about 0.1 eV is a subtle feature and beyond the accuracy of the present approach, not so much because of the underlying quantum chemical method, i.e., CC2 response theory, but because of the MM environment based on far-reaching point charges. Test calculations, performed in the context of the present work reveal that modifications of charges quite far from the FMN chromophore still have an appreciable influence on the excitation energies. Moreover, the vertical excitation energies given in Table 3 represent just one minimized configuration, whereas an ensemble average of excitation energies would be needed for a direct comparison with experiment (cf., e.g., ref 79). Due to these reasons we cannot claim to really pick up the measured red-shift of 10 nm with the methodology utilized here. However, our calculations clearly show a significant increase

(79) Hoffmann, M.; Wanko, M.; Konig, P. S. P.; Frauenheim, T.; Schulten, K.; Thiel, W.; Tajkhorshid, E.; Elstner, M. *J. Am. Chem. Soc.* **2006**, *128*, 10808.

***Table 3.*** TD-DFT and CC2 Response Vertical Excitation Energies (in eV) Calculated at QM/MM Optimized Dark, Q51-*E*, and Q51-*Z* Structures[a]

| | | TD-DFT/B3LYP | | TD-DFT/BHLYP | | CC2 | |
|---|---|---|---|---|---|---|---|
| structure | QM set | LE | CT | LE | CT | LE | CT |
| dark | A | 2.81 (0.179) | 1.860 (0.000) | 3.290 (0.269) | 3.170 (0.001) | 2.992 | 3.596 |
| Q51-*E* | A | 2.900 (0.108) | 1.833(0.000) | 3.300 (0.249) | 3.240 (0.000) | 2.996 | 3.656 |
| Q51-*Z* | A | 2.699 (0.037) | 0.947 (0.000) | 3.175 (0.176) | 2.366(0.000) | 2.923 | 2.732 |
| dark | B | 2.872 (0.100) | 1.645 (0.000) | 3.338 (0.286) | 3.167(0.000) | 3.031 | 3.627 |
| Q51-*E* | B | 2.900 (0.108) | 1.833 (0.000) | 3.356(0.295) | 3.310 (0.000) | 3.047 | 3.695 |
| Q51-*Z* | C | 2.736 (0.074) | 1.105(0.000) | 3.182 (0.238) | 2.528 (0.000) | 2.924 | 2.873 |

[a] LE and CT represent the local excitation within FMN and the CT excitation from Tyr-9 to FMN, respectively. Oscillator strengths are shown in parentheses. QM set A is the default specification for the QM region of our QM/MM calculations. For the calculations involving the QM sets B (A + Asn-33) and C (A + Asn-33 + Trp-92) the related ground-state geometries were reoptimized accordingly (see text).

in the electron density at the N5 position on going from the ground to he LE excited state (see Figure 6). On the basis of this fact one may anticipate that the experimentally observed 10 nm shift is related to changes in the H-bonds involving this atom of FMN.

**3.7.2. Charge-Transfer State (Tyr-9 → FMN).** The TD-DFT values exhibit a substantial drop in the energy of the CT state on going from the dark to the Q51-*Z* geometry. However, the CT state energies are considerably underestimated (particularly so for the B3LYP functional for reasons mentioned above) such that the gap between the LE and the CT states at the Q51-*Z* geometry becomes rather large. Furthermore, no conical intersection is predicted by TD-DFT. We conclude that TD-DFT alone is not able to provide a qualitatively correct picture of the photophysical behavior of the BLUF domain. CC2 response, on the other hand, certainly provides a qualitatively correct picture of the energetics of the low-lying LE and CT states in BLUF domains. According to Table 3 CC2 response yields a decrease in the energy of the CT state by almost 0.9 eV on going from the dark to the Q51-*Z* geometry. For the dark geometry the CT state is energetically *above* the LE state with a gap of 0.6 eV, whereas for the Q51-*Z* geometry the CT state is 0.2 eV *below* the LE state. Evidently, the CT state is much more stable in the Q51-*Z* than in the dark geometry. It is tempting to assume that also the Franck−Condon point of the signaling state (Q51-*Z* geometry) is located close to a conical intersection seam between the LE and the CT surfaces, which is populating the CT state via the LE state upon photoexcitation. Consequently, the CT state would be also instrumental for the photocycle initiated by the photoexcitation of the signaling state of the BLUF domain (vide infra).

Zirak and co-workers have observed a lower fluorescence efficiency and a shortened fluorescence lifetime in the signaling state (compared with the dark/receptor state) of BlrB,[24] AppA[21] and Slr1694[28] BLUF domains. These data support our hypothesis of the above-mentioned conical intersection near the Q51-*Z* geometry. Additionally, the ultrafast transient absorption spectroscopy measurements by Toh et al.[76] indicate a much faster photocycle in the light-adapted form of the AppA BLUF domain. In fact, no FMN anionic semiquinone ($FMN^{\bullet -}$) was observed in this work, and the authors report on the formation of flavin neutral semiquinone within some picoseconds after photoexcitation, followed by ground-state recovery (relaxation down to the signaling state conformation) after 60 ps.

The Q51-*Z* geometry may explain a much faster photocycle by faster proton transfer steps due to stronger hydrogen bonds. The relatively weak H-bond between FMN-N5 and $NH_2$ of Gln-51 in the dark state is replaced in the Q51-*Z* geometry by a stronger H-bond involving the hydroxy group of the *Z*-tautomer of Gln-51, which is more acidic, in the signaling state. Upon activation of the CT state in the Q51-*Z* conformation it is more probable that a concerted proton transfer from Tyr-9/OH to Gln-51/O$\varepsilon$ and from Gln-51/OH to FMN-N5 takes place. This assumption can be justified by the fact that such a concerted proton transfer step, in contrast to the case of dark state, is mediated via a single atom, namely, the O$\varepsilon$ of Gln-51. One may assume further that such a concerted motion would occur even faster than the $P_1 + P_2$ proton transfer steps discussed for the dark structure, hence explaining the difficulty Toh et al. had observing the FMN anionic semiquinone ($FMN^{\bullet -}$).[76] After this biradical formation the NH group of Gln-51 is still within a (somewhat weak) hydrogen-bonding network involving FMN-O4 and Trp-92. The orientation of the NH group prevents it from acting as a H acceptor, since the lone pair of the Gln-nitrogen (N$\varepsilon$) atom, pointing toward Trp-92, is already involved in a H-bonding interaction with the latter. For the radical recombination process to occur, the hydrogen atom at N5 is transferred back to Tyr-9-OH (again) via a possibly concerted hydrogen atom transfer in the opposite direction to that inducing the biradical in the first place, i.e., FMN-N5 → Gln-51-O$\varepsilon$ and Gln-51-O$\varepsilon$ → Tyr-9-OH. This last mentioned mechanism is probably more compatible with experimental observations since other biradical recombination paths may well involve larger conformational changes (on a longer time scale) such as the rotation of Gln-51 or the dislocation of Tyr-9, etc.

There is a further CT state, namely, Trp-92 → FMN, which is of some importance. At the Q51-*Z* geometry where the distance between FMN and Trp-92 is substantially decreased relative to the Met-in dark-state structure it constitutes the lowest electronically excited state with a CC2 vertical excitation energy of 2.618 eV. The corresponding value for the Tyr-9 → FMN CT state amounts to 2.873 eV (cf., Table 3). TD-DFT excitation energies for the Trp-92 → FMN CT state amount to 2.17 eV (BHLYP) and 0.84 (B3LYP), again significantly underestimating the CC2 value (in particular for the latter functional). The oscillator strength of this CT state, calculated both at the level of TD-DFT and CC2, is essentially zero. Consequently, direct population via photoexcitation is not possible and the LE state has to be involved (possibly via conical intersection). Since the Tyr-9 → FMN CT state is energetically closer to the LE state (actually rather close, cf., Table 3), one can anticipate that the Tyr-9 moiety still is the primary electron donor in the signaling state of BLUF domains and the Trp-92 most probably is playing a secondary role. Interestingly, Gauden et al.[22] suggested the possibility of a competition between the two CT processes discussed here. The photocycle of BLUF domains in the signaling state is subject of further research in our group.

***Table 4.*** Stretch and Bend Mode Frequencies (in $cm^{-1}$) for the Dark, Q51-*E*, and Q51-*Z* Structures Calculated at the B3LYP/MM Level of Theory

| | FMN modes | | | | Gln-51 modes | | | |
|---|---|---|---|---|---|---|---|---|
| structure | C4═O4[a] | C2═O2[a] | N1−C10 | C4a−N5/C10 | C═O[b] | C═N | $NH_2$ bend | QM region |
| dark | 1797.8 | 1745.3 | 1590.7 | 1656.9 | 1716.3 | | 1653.4 | B |
| Q51-*E* | 1795.2 | 1736.7 | 1600.4 | 1662.6 | | 1760.3 | | B |
| Q51-*Z* | 1791.0 | 1737.3 | 1597.9 | 1656.3 | | 1773.4 | | C |

[a] The C4═O4 and C2═O2 stretch modes contain a significant fraction of the N3−H3 stretch coordinate. [b] The C═O mode in Gln-51 contains a significant fraction of the $NH_2$ bend coordinate.

**3.8. QM/MM Vibrational Frequency Calculation.** Apart from the calculations of vertical excitation energies discussed above, also QM/MM harmonic vibrational frequencies in the electronic ground state were computed at the three geometries dark, Q51-*E*, and Q51-*Z*, respectively. The resulting values for the C4═O4 stretch mode are given in Table 4. The biradical recombination process outlined in this contribution leads to the Q51-*E* geometry (Gln-51 in imidic form), for which no substantial strengthening of the H-bond network involving FMN-O4 is taking place. The calculated shift of the FMN C4═O4 stretch mode relative to the dark geometry therefore is rather small (cf., Table 4). At the first sight this appears to be in contradiction with the experiments measuring a red-shift of about 10 $cm^{-1}$ of the FMN C4═O4 stretch mode on going from the dark to the signaling state of the BLUF domain. However, a recent FT-IR study by Stelling et al. on AppA BLUF domains[41] reveals that this shift does not appear in the first 2 ns after photoexcitation of the dark-adapted structure, whereas the biradical recombination is reported to be completed within 2−3 ns in the AppA[78] and Slr1694[32] BLUF domains. This implies that the strengthening of the H-bond network involving FMN-O4 at the O4 position and the formation of the intermediate arrived at after biradical recombination (the Q51-*E* geometry proposed here) are two separate steps occurring at different times in the photocycles, i.e., the strengthening of the H-bond network occurs *later* than the formation of the Q51-*E* geometry. Yet this is in excellent agreement with our frequency calculations, where the final Q51-*Z* geometry, i.e., our postulated signaling state geometry, exhibits basically the experimentally observed shift (7 vs 10 $cm^{-1}$ reported in ref 41) We note in passing that for the alternative mechanism involving rotation of the Gln-51 moiety a much larger shift of 40 $cm^{-1}$ was computed for the corresponding final signaling state.[40]

Further stretch and bend modes calculated in the context of the present work are shown in Table 4. The C2═O2 stretch mode, also showing a red-shift upon transition to the signaling state, is lower than that of C4═O4 which is in line with experimental observations.[20,41] A further agreement with experiment is the rather high contribution of the FMN N3−H3 stretch coordinates to both of these carbonyl modes.[20,41] The C═O mode of Gln-51, also shown in Table 4, includes significant contributions from the $NH_2$ bend coordinates of this residue. The band measured at 1653 $cm^{-1}$ is assigned to the $NH_2$ bend mode of Gln-51 which also has a significant component of the C═O stretch coordinate of the latter residue. This mode is however not present in the Q51-*E* and Q51-*Z* structures, where the Gln-51 side chain is in its imidic form. More accurate QM/MM calculations at a higher level of theory (e.g., MP2) are necessary for a more robust assignment of these modes to the measured IR bands.

## 4. Conclusions

In this article a general and conclusive mechanism for the formation of the signaling state in BLUF domains is proposed, which is compatible with the experimental results published so far for various BLUF domains in different proteins. We thus anticipate that the presented mechanism is valid for the whole range of this important class of photoreceptor proteins.

Extensive QM/MM calculations were performed, applying also high-level ab initio methods like coupled cluster (CC2) response theory in order to lay out the reaction path leading from the dark state to the signaling state structure after initial photoexcitation of the former. A Tyr-9 → FMN CT state is populated via conical intersection after triggering an electronically local excited state of the FMN subunit. The latter has, in contrast to the CT state, a rather large oscillator strength. Populating CT states, which usually have only low oscillator strength, via conical intersection appears to be a common way to achieve photoinduced charge transfer, at least for systems based on flavin.

The reaction cascade then proceeds downhill on the CT surface, inducing two proton transfer steps, and finally leads via a second conical intersection to a nonzwitterionic ground-state biradical. These two proton transfer steps transform the Gln-51 moiety, the key player in this whole mechanism, to its imidic tautomer. Biradical recombination, a further step in the cascade, then transforms this tautomer to the *E*-isomer (*E*-form). A subsequent second isomerization, triggered by the exchange of the Met-94 and Trp-92 residues in its vicinity further stabilizes the imidic form of Gln-51 (*Z*-form). Accompanied by this *flip* is a spatial dislocation of the Asn-33 residue, moving closer to the FMN chromophore. It turns out to be this effect that is mainly responsible for the experimentally observed red-shift in the flavin C4═O4 stretch frequency.

The thermal back-reaction from the long living signaling state involves the back-tautomerization of Gln-51. The related barrier is estimated to be rather high, particularly so, if the imidic tautomer is stabilized in the *Z*-form after the interchange of Met-94 and Trp-92. We assume that this Met-94 versus Trp-92 flip actually is the trigger for the large conformational change of the protein transmitting the signal to the biological environment. In its dark state and under aerobic conditions, AppA binds to purple bacteria photosystem regulator (PpsR), a transcription factor (hence forming a complex which is not able to bind to DNA) and therefore initiates gene expression. The oligomerization state of AppA changes in its light-induced signaling state,[80] but the mechanism of PpsR release, leading to gene expression inhibition, is not fully known. The mechanism proposed here also provides a hint for the role of the strictly conserved Met-94 residue next to Gln-51. Methionine is the

(80) Hazra, P.; Inoue, K.; Laan, W.; Hellingwerf, K. J.; Terazima, M. *J. Phys. Chem. B* **2007**, *112*, 1494.

only amino acid which can only act as a H acceptor; hence, it forms an attractive interaction with Gln-$NH_2$ but is repulsive toward the proposed Gln-*Z* isomer.

None of the reaction steps presented here do involve any rotation of the Gln-51 side chain. Rotation of Gln-51 was previously postulated by others to play a key role in the mechanism, but the present study shows that the barriers of rotation are considerably higher than those of direct proton transfer as conjectured here. Interestingly, the mechanism implies only photoisomerization of the protein environment but not of the FMN itself. The FMN chromophore just plays the role of an antenna and mediator for the tautomerization and subsequent isomerization of Gln-51. This, to our knowledge, is unique for biological photoreceptors.

**Acknowledgment.** The authors thank Dr. Paul Sherwood for providing the CHEMSHELL QM/MM interface. This project is part of the Graduate College Sensory Photoreceptors in Natural and Artificial Systems (GRK 640) in Regensburg, funded by the Deutsche Forschungsgemeinschaft (DFG).

**Supporting Information Available:** Conservation pattern derived from 148 homologue sequences of the BLUF protein family (HMM-LOGO for PFAM PF04940 "BLUF "), CHARMM parameters used for MM description of FMN, and complete refs 13, 44, 47, and 51. This material is available free of charge via the Internet at http://pubs.acs.org.

JA803726A